

# The impact of collagen sponge composite bone marrow mesenchymal stem cells (BMSCs) in inducing interbody fusion

W.-D. ZHENG, J.-J. MING, W.-L. CHANG

Department of Orthopaedic and Trauma Surgery, Jining No. 1 People's Hospital, Jining, Shandong, China

**Abstract. – OBJECTIVE:** To assess the effectiveness of bone mesenchymal stem cells (BMSCs) in the induction of interbody fusion.

**PATIENTS AND METHODS:** The 3rd generation BMSCs were seeded on collagen sponge scaffold and cultured in osteoblast induction medium for 3 weeks to prepare cell-scaffold complex. Thirty patients were randomly divided into three groups to establish the L4/L5 interbody fusion model. The cell-scaffold complex was implanted in the intervertebral space in group I, the collagen sponge scaffold was implanted in group II, and the autologous iliac crest spongy bone was implanted in group III. Palpation, radiography, micro-CT, and histology were performed on the 12th weeks after operation to evaluate osteogenesis and spinal fusion.

**RESULTS:** BMSCs differentiated into osteoblasts in the cell-scaffold complex after osteogenic induction for 3 weeks. The spinal fusion rates in group I, II, and III were 40%, 0%, and 70%, respectively. Micro-CT and histological examination showed mature bone marrow and trabecular bone formation in the fusion segments. The new bone was integrated with the upper and lower vertebral body. The bone trabecula in group III was stronger than group I. The surgical segments in group II was scar tissue without collagen sponge residue.

**CONCLUSIONS:** BMSCs can induce osseous fusion in the lumbar vertebra.

*Key Words:*

BMSCs, Interbody fusion, Collagen sponge.

## Introduction

In recent years, bone tissue engineering has been introduced into the study of spinal fusion. Seed cells with good biological characteristics and appropriate scaffold materials are the prerequisites to obtain ideal tissue-engineered bone. Based on the in-depth investigation on stem cells, it was

found that stem cells served as a new choice of tissue-engineered seed cells. BMSCs are particularly well-researched among applicable bone-tissue engineered seed cells<sup>1,2</sup>. It was observed that new bone formed and transverse process fused on the 12<sup>th</sup> weeks after the implantation of BMSCs and scaffolds in the transverse process<sup>3</sup>. Previous studies indicated that new bone formed in the defect area tested by imaging and histology on the 8<sup>th</sup> weeks after osteoinduced BMSCs composite collagen sponge implanted in the model of patients with vertebral plate<sup>4</sup>. Thus, we seeded BMSCs in the collagen sponge scaffold and implanted them into the defect of L4/L5 interbody fusion model after three weeks' osteogenic induction. Osteogenesis and interbody fusion were assessed based on palpation, imaging, and histology.

## Patients and Methods

### *BMSCs Separation and Cultivation*

BMSCs were isolated and cultured as described by Dong et al<sup>5</sup>. Briefly, the patients were sacrificed by ear vein occlusion and immersion sterilized at a volume fraction of 75% ethanol for 10 min. The bilateral femurs were taken out and the attached soft tissues were removed. A 5 ml syringe containing 2 ml heparin was used to flush out the contents of the medullary canal to prepare single cell suspension. The obtained single cell suspension was centrifuged at 2000 g for 20 min after adding the same amount of separation liquid. The middle cell layer was washed with Dulbecco's Modified Eagle's medium (DMEM) medium (Sigma-Aldrich, St. Louis, MO, USA) and centrifuged at 1000 g for 5 min. Next, the sediment was added with cell medium containing 10% fetal bovine serum (FBS, Thermo Fisher Scientific, Waltham, MA, USA), 100 U/ml penicillin, and 100 µg/ml strep-

tomycin (Sigma-Aldrich, St. Louis, MO, USA), which was seeded in culture flask at a density of  $10^5/\text{cm}^2$  and cultured at  $37^\circ\text{C}$ , 5%  $\text{CO}_2$ , and 95% humidity. The medium was changed after 48 h. The primary monolayer cells were passaged at a ratio of 1:2 at 70-80% confluence<sup>6</sup>. All procedures were approved by the Animal Ethics Committee of Jining No. 1 People's Hospital.

#### ***Collagen Sponge Scaffold Preparation and Cell Implantation***

The sterile collagen sponge scaffold (purchased from Beijing Yilikang Bioengineering Development Center, Beijing, China) was cut into circular shapes with a diameter of 10 mm, uniformly pressed to a thickness of 2 mm, and placed in medium (without fetal calf serum) for 24 h. Then, it was placed in a 24-well plate after drying and 0.3 ml solution with  $1 \times 10^8/\text{mL}$  of P3 BMSCs cell suspension. After 2 h incubation, the same operation was repeated on the reverse side of the scaffold by adding with 0.4 ml complete medium<sup>7</sup>.

#### ***Osteoinductive Culture and Identification***

After 24 h, the complete medium was changed to a medium containing osteogenic agent (1 mmol/L sodium  $\beta$ -glycerophosphate,  $1 \times 10^{-8}$  mol/L dexamethasone, and 50 mg/L vitamin C, concentrations of 1 mmol/L) (Roche, Basel, Switzerland) for 3 weeks of culture. Cell-collagen sponge was fixed with 3% glutaraldehyde solution and washed with PBS solution for three times. The sample was immersed in isopentyl acetate after dehydration by gradient alcohol (30-100%). After that, the sample was frozen at  $-12^\circ\text{C}$  and coated by gold particles to observe cells and collagen sponge compound growth upon scanning electron microscopy. Conventional HE staining was performed for observation and photography.

#### ***Cell-Scaffold Complex Alkaline Phosphatase Staining***

Cell scaffold complex was washed by PBS twice and fixed by 40 g/L paraformaldehyde for 30 min. The detection was performed according to the manual and observed under the microscope.

#### ***Alizarin Red Staining***

Cells scaffold complex was washed for 2 times and fixed in 95% ethanol for 30 min. Next, the specimen was stained with alizarin red dye for 3 to 5 min. At last, the specimen was washed by acetone and acetone/xylene (volume ratio 1:1) and

observed under the microscope. Trypan blue staining (Solarbio, Beijing, China) was used to estimate the number of viable cells on the scaffold<sup>8</sup>.

#### ***Model Establishment and Transplantation***

Thirty patients were randomly divided into three groups (I, II, and III). The subjects were anesthetized by intraperitoneal injection of 20% Uralose (1200 mg/kg). During operation, the ventral was bolstered by  $-45^\circ$  beveled wedge-shaped soft board for manipulation facility. A 2 cm incision was made at 1 cm of the lateral transverse process parallel to the transverse process. All the operations were carried out around the fifth transverse process of the right side. L4/L5 intervertebral space and 1/2 of L4 and L5 vertebral body were exposed. The anterior L4/L5 intervertebral disc was pressed by the cannula (ID = 11 mm) and a 5 mm deep round defect was created using a flathead drill (diameter = 10 mm). After bleeding was stopped by dry gauze packing, different materials were implanted. The cell-scaffold complex was implanted in the intervertebral space in group I, the collagen sponge scaffold was implanted in group II, and the autologous iliac crest spongy bone was implanted in group III. In group I, the cell-scaffold complex was washed by PBS for three times and three complexes were implanted to each subject. In group II, the collagen sponge scaffold was immersed in complete medium for 24 h and washed by PBS for three times before implantation. A 6 mm  $\times$  8 mm spongy bone from the right iliac was cut into 1 mm<sup>3</sup> and implanted. The graft was put at the place 1 mm higher than the anterior edge of centrum. Next, the groove was covered by gelatin sponge. At last, the incision was sutured and penicillin was injected to prevent infection. A 6 mm  $\times$  8 mm spongy bone was also extracted from the right iliac of the subjects in group I and II<sup>9</sup>. All the enrolled objects have signed informed consent

#### ***X-Ray Examination***

Segments were performed on the anteroposterior plane by dual energy X-ray absorptiometry using a densitometer (QDR Discovery, Hologic, Bedford, MA, USA) operating at high-resolution mode<sup>10</sup>.

#### ***Palpation***

In the surgical plane, the supraspinal ligament and interspinous ligament were cut off. Two surgeons evaluated and scored the integration during

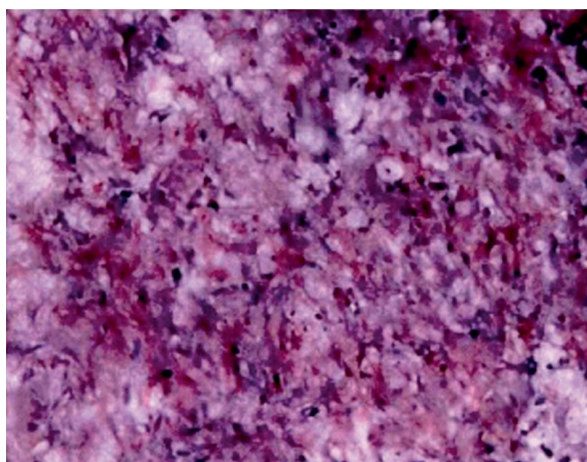


**Figure 1.** Scanning electron microscopy showed collagen sponge after 3 weeks' osteogenesis.

surgical stages. The evaluation included abdominal flexion, dorsiflexion, lateral flexion, and torsion tests. In accordance with the evaluation criteria, no false joint activity was defined as fusion success<sup>11</sup>.

#### **Micro-CT Examination**

One-half of the upper and lower vertebral bodies were scanned by Micro-CT (thickness 48  $\mu\text{m}$ ) and reconstructed (thickness 16  $\mu\text{m}$ ) to evaluate the fused segment<sup>12</sup>.

#### **Histological Examination**

The obtained specimens were fixed in 4% paraformaldehyde solution (pH7.2) for 2 weeks and decalcified by 10% EDTA for about 6 weeks. Next, the specimen was sliced for 5  $\mu\text{m}$  thickness and stained by HE for observation<sup>13</sup>.

#### **Statistical Analysis**

All data analyses were performed on SPSS 20.0 software (IBM, Armonk, NY, USA) and the measurement data were compared by the *t*-test.  $p < 0.05$  was considered as statistical significance.

## **Results**

#### **Osteogenesis Induction and Identification**

Through inverted microscope, we found that the number of cells in the stent surface was increased as the induction time extended. Moreover, the cell shape gradually transformed from spindle shape into polygons, and some cells migrated

to the scaffold pores. Data of scanning electron microscopy showed that cell clusters attached to the surface of the collagen sponge after 3 weeks cultivation (Figure 1). The cells were in polygon shape and shingles arranged. Some cells migrated into the scaffold pores, and calcium nodules could be observed on the scaffold surface. HE staining result revealed that numerous polygonal and spindle-shaped cells in the pores of scaffolds and were connected into network (Figure 2). Alkaline phosphatase staining data showed no blue-violet particles in the cells on the scaffold as strongly positive (Figure 3). By alizarin red staining, our study demonstrated flaky red nodules located in the out of cytoplasm (Figure 4).

#### **X-Ray Examination and Palpation**

No kyphosis or deformity was found by X ray examination on 12 weeks after surgery. 4 segments were found fusions in group I (40%), 7 segments were fused in group III (70%), but no obvious new bone formation was observed in group II. Palpation demonstrated that the fusion rates of the three groups were 40% in group I, 0% in group II, and 70% in group III. Bone fusion exhibited in the intervertebral bone, with mature bone, clear trabecular bone and marrow cavity. The integration between the new bone and vertebral body was also presented. The fused intervertebral trabecular in group III was thicker and denser than that in group I. New bone formation was also found in the unfused intervertebral space in group I and III. There was soft tissue filling between the new bone or between the new bone and the vertebral

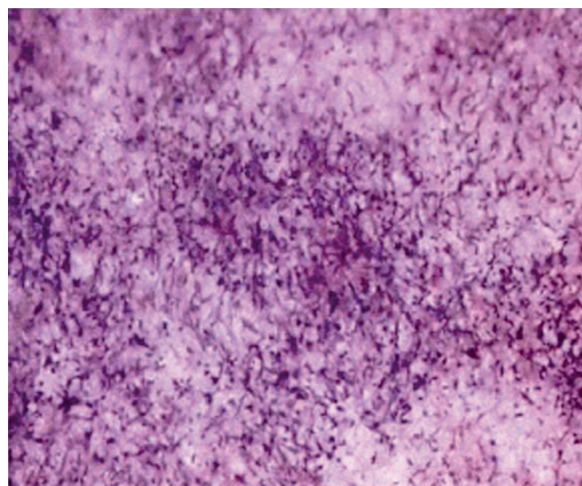


**Figure 2.** HE staining showed collagen sponge scaffold after 3 weeks' osteogenesis.

**Table I.** X-ray examination on the 12th week after operation (n, %).

Group	Bone fusion (n)	Fusion rate (%)
Group I	10	40
Group II	0	0
Group III	7	70

body. However, no new bone was formed in the group II. Histological examinations were basically the same as the results of micro-CT. Mature neo-bone was found in the fusion segments in group I and group III. The bone tissue in group III was more mature compared with that in group I, which showed integrated vertebral bodies and a small amount of new bone formation in the unfused disc space. The defects in group II were filled with collagen tissue, whereas new bone formation was shown. Also, no collagen sponge residue was found in all segments (Table I).

### Discussion

Clinically, the mechanism of spine fusion and its complications receive more in-depth understanding, and the corresponding patient model is more widely used in spine surgery<sup>12</sup>. Meanwhile, recent researches confirmed that spinal fusion model is of great significance in the evaluation of the role of tissue engineering and gene therapy. In the investigation of spinal fusion, the researchers also used a variety of different experimental patient models and for different fusion sites and types<sup>13</sup>. For example, the *in vivo* model used in anterior interbody fusion varies from rodent to primate rhesus monkeys. Mouse is the most commonly used experimental subjects at present. However, the limitation still exists that spine and vertebral body of mice was smaller, which was difficult to adopt fixation between the vertebral bodies. Additionally, the spontaneous fusion occurs after disc resection<sup>14</sup>. This study used forstner bit to open the bone groove, so as to solve the problem of operational difficulties and spontaneous fusion in the mouse model<sup>15</sup>. Our results showed that there was no interbody fusion in the blank group, which confirmed that the experimental methods used in this study presented no drawbacks of spontaneous fusion. Moreover, no significant deformity was found in the bony fusion site and the surgical site, suggesting that the operation used in this study would not disrupt the stability of the spine<sup>16</sup>. The

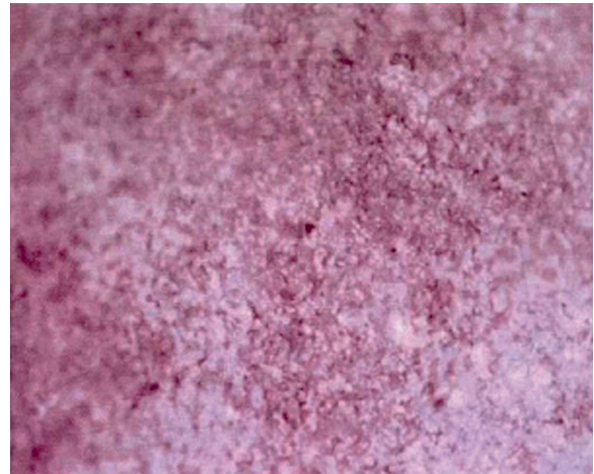


**Figure 3.** Alkaline phosphatase staining showed negative cell response after 3 weeks' osteogenesis.

above results demonstrate that collagen sponge composite bone marrow mesenchymal stem cells induce interbody fusion model, which is of great significance to the exploration of anterior interbody fusion, especially in the cytokines, cells, and genes to promote interbody fusion<sup>17</sup>. However, in the autologous bone group and the experimental group, some of the bone formed segments failed to fuse, which may be caused by the unrigid fixation of the surgical segment, thus limiting the further formation of the bone and the interbody fusion<sup>17</sup>. BMSCs composite calcium phosphate ceramics was applied in the lumbar posterolateral fusion test of patients and evaluated the effects by manual palpation, CT, and histological methods<sup>18</sup>. The results showed that the spinal fu-

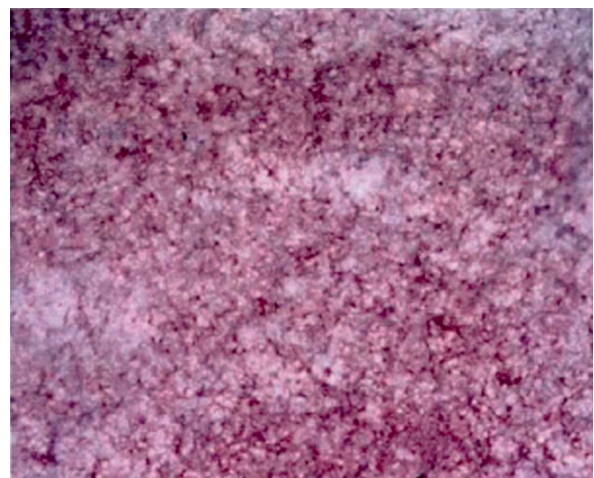


**Figure 4.** Alizarin red staining showed calcium deposition after 3 weeks' osteogenesis.

sion rate was much higher than that of autologous bone transplant group. In a comparative study<sup>19</sup>, it was found that the fusion rate of BMSCs composite hydroxyapatite was 80% and that of pure hydroxyapatite was only 40%. In another comparative study<sup>20</sup>, it was revealed that the fusion rate of the posterior lateral fusion with BMSCs was only 33%, and the fusion rate after differentiation was increased to 80%. Histology demonstrated that the trabecular bone of the latter was significantly thicker than the former intervertebral disc.

## Conclusions

We demonstrated that collagen sponge composite BMSCs induced osseous fusion in the lumbar vertebra, which is worthy of clinical popularization.

## Acknowledgments

This work was supported by the Natural Science Foundation of Shandong province (No. ZR2015HL086).

## Conflict of Interest

The Authors declare that they have no conflict of interest.

## References

- MEHMOOD A, ALI M, KHAN SN, RIAZUDDIN S. Diazoxide preconditioning of endothelial progenitor cells improves their ability to repair the infarcted myocardium. *Cell Biol Int* 2015; 39: 1251-1263.
- CHU ZM, LI HB, SUN SX, JIANG YC, WANG B, DONG YF. Melatonin promotes osteoblast differentiation of bone marrow mesenchymal stem cells in aged rats. *Eur Rev Med Pharmacol Sci* 2017; 21: 4446-4456.
- JIN M, CHEN Y, ZHOU Y, MEI Y, LIU W, PAN C, HUA X. Transplantation of bone marrow-derived mesenchymal stem cells expressing elastin alleviates pelvic floor dysfunction. *Stem Cell Res Ther* 2016; 7: 51.
- SOUZA MC, SILVA JD, PADUA TA, TORRES ND, ANTUNES MA, XISTO DG, ABREU TP, CAPELOZZI VL, MORALES MM, SA PINHEIRO AA, CARUSO-NEVES C, HENRIQUES MG, ROCCO PR. Mesenchymal stromal cell therapy attenuated lung and kidney injury but not brain damage in experimental cerebral malaria. *Stem Cell Res Ther* 2015; 6: 102.
- DONG X, ZHU F, LIU Q, ZHANG Y, WU J, JIANG W, ZHANG L, DONG S. Transplanted bone marrow mesenchymal stem cells protects myocardium by regulating 14-3-3 protein in a rat model of diabetic cardiomyopathy. *Int J Clin Exp Pathol* 2014; 7: 3714-3723.
- TENG C, ZHOU C, XU D, BI F. Combination of platelet-rich plasma and bone marrow mesenchymal stem cells enhances tendon-bone healing in a rabbit model of anterior cruciate ligament reconstruction. *J Orthop Surg Res* 2016; 11: 96.
- DAI L, HU X, ZHANG X, ZHU J, ZHANG J, FU X, DUAN X, AO Y, ZHOU C. Different tenogenic differentiation capacities of different mesenchymal stem cells in the presence of BMP-12. *J Transl Med* 2015; 13: 200.
- NG J, WEI Y, ZHOU B, BURAPACHAISRI A, GUO E, VUNJAK-NOVAKOVIC G. Extracellular matrix components and culture regimen selectively regulate cartilage formation by self-assembling human mesenchymal stem cells in vitro and in vivo. *Stem Cell Res Ther* 2016; 7: 183.
- GERAGHTY S, KUANG JQ, YOO D, LEROUX-Williams M, Vangness CT, Jr., Danilkovitch A. A novel, cryopreserved, viable osteochondral allograft designed to augment marrow stimulation for articular cartilage repair. *J Orthop Surg Res* 2015; 10: 66.
- LIU CC, TIAN FM, ZHOU Z, WANG P, GOU Y, ZHANG H, WANG WY, SHEN Y, ZHANG YZ, ZHANG L. Protective effect of calcitonin on lumbar fusion-induced adjacent-segment disc degeneration in ovariectomized rat. *BMC Musculoskelet Disord* 2015; 16: 342.
- REA S, STEVENSON A, GILES NL, WOOD FM, FEAR MW. Cells from the hematopoietic lineage are only present transiently during healing in a mouse model of non-severe burn injury. *Stem Cell Res Ther* 2015; 6: 134.
- JANG Y, JUNG H, NAM Y, RIM YA, KIM J, JEONG SH, JU JH. Centrifugal gravity-induced BMP4 induces chondrogenic differentiation of adipose-derived stem cells via SOX9 upregulation. *Stem Cell Res Ther* 2016; 7: 184.
- KANETO CM, LIMA PS, ZANETTE DL, OLIVEIRA TY, DE ASSIS PEREIRA F, LORENZI JC, DOS SANTOS JL, PRATA KL, NETO JM, DE PAULA FJ, SILVA WA, JR. Osteoblastic differentiation of bone marrow mesenchymal stromal cells in Bruck Syndrome. *BMC Med Genet* 2016; 17: 38.
- ZHOU X, WANG J, SUN H, QI Y, XU W, LUO D, JIN X, LI C, CHEN W, LIN Z, LI F, ZHANG R, LI G. MicroRNA-99a regulates early chondrogenic differentiation of rat mesenchymal stem cells by targeting the BMP2 gene. *Cell Tissue Res* 2016; 366: 143-153.
- KATAGIRI W, OSUGI M, KAWAI T, HIBI H. First-in-human study and clinical case reports of the alveolar bone regeneration with the secretome from human mesenchymal stem cells. *Head Face Med* 2016; 12: 5.
- ORTH P, CUCCHIARINI M, ZURAKOWSKI D, MENDER MD, KOHN DM, MADRY H. Parathyroid hormone [1-34] improves articular cartilage surface architecture and integration and subchondral bone reconstitution in osteochondral defects in vivo. *Osteoarthritis Cartilage* 2013; 21: 614-624.
- PELIZZO G, AVANZINI MA, ICARO CORNAGLIA A, OSTI M, ROMANO P, AVOLIO L, MACCARIO R, DOMINICI M, DE SILVESTRI A, ANDREATTA E, COSTANZO F, MANTELLI M, INGO

- D, PICCINNO S, CALCATERRA V. Mesenchymal stromal cells for cutaneous wound healing in a rabbit model: pre-clinical study applicable in the pediatric surgical setting. *J Transl Med* 2015; 13: 219.
- 18) REPEL L, SCHIAVI J, CHARIF N, LEGER L, YU H, PINZANO A, HENRIONNET C, STOLTZ JF, BENSOUSSAN D, HUSELSTEIN C. Chondrogenic induction of mesenchymal stromal/stem cells from Wharton's jelly embedded in alginate hydrogel and without added growth factor: an alternative stem cell source for cartilage tissue engineering. *Stem Cell Res Ther* 2015; 6: 260.
- 19) MCCORRY MC, PUETZER JL, BONASSAR LJ. Characterization of mesenchymal stem cells and fibrochondrocytes in three-dimensional co-culture: analysis of cell shape, matrix production, and mechanical performance. *Stem Cell Res Ther* 2016; 7: 39.
- 20) HAYRAPETYAN A, BONGIO M, LEEUWENBURGH SC, JANSEN JA, VAN DEN BEUCKEN JJ. Effect of nano-HA/collagen composite hydrogels on osteogenic behavior of mesenchymal stromal cells. *Stem Cell Rev* 2016; 12: 352-364.
- 21) MENG F, XU L, HUANG S, LIU Y, HOU Y, WANG K, JIANG X, LI G. Small nuclear ribonucleoprotein polypeptide N (Sm51) promotes osteogenic differentiation of bone marrow mesenchymal stem cells by regulating Runx2. *Cell Tissue Res* 2016; 366: 155-162.
- 22) LANE AM, TOTTERDELL P, MACDONALD I, DEVONPORT TJ, FRIESEN AP, BEEDIE CJ, STANLEY D, NEVILL A. Brief online training enhances competitive performance: findings of the BBC lab UK psychological skills intervention study. *Front Psychol* 2016; 7: 413.